

A New Species of Free-living Marine Nematode (*Ptycholaimellus*: Chromadoridae: Chromadorida: Nematoda) from Mangrove Wetlands in China

Yi-Jia Shih^{1,2} , Yu-Zhen Chen¹, and Yu-Qing Guo^{1,2,*}

¹Fisheries College, Jimei University, Xiamen 361021, China. *Correspondence: E-mail: guoyuqing@jmu.edu.cn (Guo).
E-mail: eja0313@gmail.com (Shih); yifangch2012@163.com (Chen)

²Fujian Provincial key Laboratory of Marine Fishery Resources and Eco-environment, Jimei University, Xiamen 361021, China

Received 19 October 2021 / Accepted 2 March 2022 / Published 26 May 2022
Communicated by John Wang

This study presents a new species of free-living marine nematode, *Ptycholaimellus luoyang* sp. nov., from mangrove wetlands in China. The identification was confirmed by analyzing morphological characteristics and three genes: *COI*, 18S rDNA, and 28S rDNA. This species is distinguished from allied species by its short cephalic setae, cylindrical pharynx with anterior swelling, sclerotized transverse ridges occurring near the dorsal tooth, rod-like gubernaculum and proximal, arch-like, slightly waved, middle curved, and distally pointed spicules. The Bayesian topology was regarded as morphological evidence of *P. luoyang* sp. nov. being a distinct species. Interspecific and intrageneric thresholds of the K2P distance divergence have been presented here for the first time.

Key words: Free-living marine nematode, *Ptycholaimellus*, New species, Morphology, DNA barcoding.

BACKGROUND

Free-living marine nematodes are globally abundant organisms, comprising up to 99% of the meiofaunal community in benthic environments (Bhadury et al. 2008; Derycke et al. 2010; Pitusi et al. 2021; Ridall and Ingels 2021). Their densities can exceed 10,000 individuals per 10 cm² (Ridall and Ingels 2021). They play a key role in nutrient cycling and affect carbon fixation in mangrove wetlands (Ferris 2010; Naidoo et al. 2021). Hence, the identification of nematode species improves our understanding of an ecosystem's functional roles (Bhadury et al. 2008; Sahraean et al. 2017).

Ptycholaimellus is a cosmopolitan genus in mangrove wetlands around the world (Nicholas et al. 1991; Rzeznik-Orignac et al. 2003; Mokievsky et al. 2011; Yang et al. 2019). This genus differs from allied

genera due to distinct characteristics in the structure of the cephalic anatomy, in particular the buccal cavity, amphids and esophageal bulb (Jensen and Nehring 1992; Wang et al. 2015; Huang and Gao 2016). Thus far 22 species have been described, all of which are organized in a key by Huang and Gao (2016). Moreover, the fauna of this genus known thus far from China include *P. adocius* Dashchenko & Belogurov 1984, *P. longibulbus* Wang, An & Huang, 2015, *P. macrodentatus* Timm, 1961, *P. ocellus* Huang & Wang, 2011, and *P. pirus* Huang & Gao, 2016.

Although morphologic identification is a traditional method, DNA barcoding may provide a faster and more effective method for nematode identification (Derycke et al. 2010). Three genes, *COI*, 18S rDNA, and 28S rDNA, have recently been established as key taxonomic characteristics for nematodes (Blaxter et al. 1998; Derycke et al. 2010; Leduc and Zhao 2021).

However, the current sequence database for marine nematodes remains incomplete, and a substantial number of misidentified organisms remain (Pitusi et al. 2021). The correct identification of species and their nucleotide sequences would allow the construction of a reference database for further studies.

Here, we report the identification of a new species, *P. luoyang* sp. nov., from mangrove wetlands in three provinces of China. The diagnosis of characteristics were described, and three key genes were sequenced. This was also done for *P. adocius* to confirm the phylogenetic placement of the new species.

MATERIALS AND METHODS

Sample collection, meiofauna extraction, and nematode identification

The nematode species were collected from undisturbed sediment at four locations: Luoyang River estuary in Quanzhou City, Fujian Province (118.69°E; 24.95°N) in April 2017; Xinying Port in Danzhou City, Hainan Province (109.16°E; 19.46°N) in December 2020; Neilingding Futian National Nature Reserve in Shenzhen City, Guangdong Province (114.01°E; 22.31°N) in November 2020; and Jiulong River estuary in Zhangzhou City, Fujian Province (117.95°E; 24.45°N) in July 2021. Sediment sampling and nematode extraction were performed as described in our previous studies (Guo et al. 2015; Yang et al. 2019 2020). Part of the samples were fixed with 5% formalin for species identification. Permanent slides were prepared as described by Huang and Gao (2016). The holotype and paratypes were deposited into the Jimei University, Xiamen, China.

Part of the samples were placed in a refrigerator at -20°C for DNA extraction. The slides were prepared for species identification as follows: (1) make a paraffin

ring on the glass slide; (2) drop 5% glycerin in the center of the paraffin ring; (3) transfer the individual nematode into the glycerin; (4) cover it with a cover glass and heat until the paraffin has melted; (5) after identification, place the slide on the heater and remove the cover glass; (6) transfer the nematode to the tube for DNA extraction.

DNA extraction and PCR amplification

Twelve individual nematodes were prepared for total genomic DNA extraction using the Tiangen Dp324-03 DNA Isolation Kit. The modified manufacturer's instructions are described as follows: (1) mix 20 µl GA buffer with an individual nematode in a 1.5 ml microcentrifuge tube, vortex for 15 seconds; (2) add 5 µl proteinase K (20 mg/ml), vortex for a few seconds, and incubate at 55°C for an hour; (3) add 20 µl GB buffer and incubate at 70°C for 10 minutes; (4) add 20 µl 99% ethanol, and vortex for 15 seconds; (5) transfer the mixture into the spin columns CB3, centrifuge at 12,000 rpm for 30 seconds, discard the liquid and replace the spin column; (6) add 50 µl GD buffer, centrifuge at 12,000 rpm for 30 seconds, discard the liquid, and replace the collection tube; (7) add 60 µl PW buffer, centrifuge at 12,000 rpm for 30 seconds, discard the liquid, replace the collection tube and repeat this step; (8) centrifuge at 12,000 rpm for 2 minutes to dry the membrane completely; (9) attach the spin column to a new collection tube, add 30 µl TE buffer, centrifuge at 12,000 rpm for 2 minutes for total genomic DNA elution.

Three genes, *COI*, 18S rDNA, and 28S rDNA, were selected for genetic analysis. The primers used in this analysis are presented in table 1. Each reaction was performed in a 25 µl solution, including 6 µl DNA template, 12.5 µl 2X Pro Taq Master Mix, 0.5 µl for each forward and reverse primer and 5.5 µl distillation H₂O. PCR cycling conditions were described by

Table 1. Primers used for genetic analyses

Primer	Gene region	Sequence (5'-3')	References
JB3F	<i>COI</i> gene	F- TTT TTT GGG CAT CCT GAG GTT TATR	Derycke et al. 2010
JB5R		R- AGC ACC TAA ACT TAA AAC ATA ATG AAA ATG	
LCO	<i>COI</i> gene	GGT CAA CAA ATC ATA AAG ATA TTG G	Derycke et al. 2010
HCO		R- TAA ACT TCA GGG TGA CCA AAA AAT CA	
MN18F	18S rDNA	F- CGC GAA TRG CTC ATT ACA ACA GC	Bhadury et al. 2008
Nem_18S_R		R- GGG CGG TAT CTG ATC GCC	
MN18F	18S rDNA	F- CGC GAA TRG CTC ATT ACA ACAGC	Bhadury et al. 2006
22R		GCC TGC TGC CTT CCT TGG A	
D2A	28S rDNA	F- ACA AGT ACC GTG AGG GAA AGT TG	De Ley et al. 2005
D3B		R- TCG GAA GGA ACC AGC TAC TA	

Derycke et al. (2010). Following the PCR assay, 5 µl of each PCR product was separated by electrophoresis on a 1% agarose gel. The gel was stained with 0.5 µg/ml ethidium bromide, and imaged using an ultraviolet transillumination system. All positive PCR amplicons were sequenced by Sangon Biotech, Ltd.

Sequencing and analyses

Twelve fragments of each gene were obtained from individual *P. iuncturam* sp. nov. and *P. adocius* nematodes in this study. All sequences were deposited in GenBank, and the reference sequences were selected for phylogenetic analysis. Intrageneric species plus *Hypodontolaimus inaequalis* and *Terschellingia longicaudat*, of allied genus and outgroup, respectively, were included. GenBank accession numbers are presented in table 2. Each gene sequence was analyzed and modified, with default gap penalties, as separate alignments using CLUSTAL-W program by BioEdit version 7.2.3. Subsequently, three fragments were selected from different individuals and combined for phylogenetic analysis. Bayesian inference (BI) analyses of the combined dataset, using the MrBayes v3.2.6 program, produced phylogenetic trees. Metropolis coupled Markov chain Monte Carlo analyses were run for 1,500,000 generations, and one tree was sampled every 500 generations. The standard deviation of split frequencies converged to a value of 0.05. The BI posterior probability for clades was only displayed when exceeding 0.90. Moreover, interspecific and intraspecific thresholds based on three gene segments were calculated using Kimura 2-parameter distances (K2P) via MEGA 7.0 software. The parameter model

was reconstructed with 1,000 bootstrap replicates.

Terminology and abbreviations

Measurements are in provided in µm. Abbreviations are as follows: a, body length divided by maximum body diameter; b, body length divided by pharyngeal length; c, body length divided by tail length; a.b.d., anal body diameter; c.d., corresponding diameter; V, distance of vulva from anterior end; V%, position of vulva from anterior end as a percentage of body length; Spic, spicule length along arch.

RESULTS

TAXONOMY

Family Chromadoridae Filipjev, 1917 Genus *Ptycholaimellus* Cobb, 1920

Ptycholaimellus luoyang sp. nov.

(Figs. 1A–G; 2A–E; Table 3)

urn:lsid:zoobank.org:act:DF62ED83-B149-41B1-9A64-63850F9683B7

Material examined: Holotype: one male (♂ 1: QZLYJ201704262U1002); Paratypes: four males (♂ 2: QZLYJ201704262U2004, ♂ 3: QZLYJ201704261D1010, ♂ 4: QZLYJ201704262U2001, ♂ 5: QZLYJ201704261M2002), two females (♀ 1: QZLYJ201704262U3003, ♀ 2: QZLYJ201704263D1001), one juvenile (QZLYJ201704261U2004). All specimens were collected from the Luoyang River estuary in

Table 2. GenBank accession numbers and reference species

No.	Species	GenBank accession number		
		COI	18S rDNA	28S rDNA
1	<i>Hypodontolaimus inaequalis</i>	MG659396.1	MG669814.1	-
		MG659395.1	MG669813.1	-
2	<i>Ptycholaimellus luoyang</i> *	MZ779078	MZ779185	MZ779190
3	<i>Ptycholaimellus luoyang</i> *	MZ779080	MZ779197	MZ779195
4	<i>Ptycholaimellus adocius</i> *	MZ779079	MZ779198	MZ779193
5	<i>Ptycholaimellus adocius</i> *	MZ779078	MZ779199	MZ779194
6	<i>Ptycholaimellus areniculus</i>	-	MG669988.1	-
		-	MG669987.1	-
7	<i>Ptycholaimellus brevisetosus</i>	MK604919.1	MK626833.1	-
8	<i>Ptycholaimellus carinatus</i>	MG659519.1	-	-
9	<i>Ptycholaimellus pandispiculatus</i>	LT795773.1	-	-
		LT795787.1	-	-
10	<i>Terschellingia longicaudata</i>	LT795770.1	-	-

Note: *indicates that the sequences were obtained in this study.

Quanzhou City, Fujian Province (118.69°E; 24.95°N) in April 2017.

Type locality and habitat: Intertidal mud sediment from a mangrove wetland in the Luoyang River estuary, Fujian Province (24.94°N, 118.67°E). Specimens present in the surface layer sediment to a depth of 0–5 cm. Total nitrogen: 1.31 mg/g; total phosphorus: 0.40 mg/g; total organic carbon: 1.72%.

Etymology: The species name refers to its first sampling location, Luoyang River.

Diagnosis: Body cylindrical (Fig. 1A), tapering acutely at posterior extremity, length 0.87–1.2 mm, with maximum body diameter 55–77 μm ($a = 15.7\text{--}19.3$). Cuticle annulated, about 6 annulus per 10 μm, and has homogeneous punctations with lateral differentiation of two longitudinal rows of coarse dots which begins at 5–7 μm from anterior end and the distance between these two longitudinal rows gradually widens from head to mid-body part and then narrows to the tail (Figs. 1B, 2A–D), except the terminal of tail about 8–12 μm without punctations nor lateral differentiation (Fig. 2B, D). Somatic setae exist near the two rows of dots. Amphids not observed. Body anterior end slightly rounded, separated from rest of body by a collar

(groove). Inner and outer labial sensillae inconspicuous. Four cephalic setae inserted on collar (Figs. 1B, 2A), length approximate 1.9–2.3 μm. Buccal cavity with an S-shaped hollow dorsal tooth, apical end of tooth hook-like. Sclerotized transverse ridges occur near the dorsal tooth (Figs. 1C, 2C). Pharynx cylindrical with anterior slightly swelling 19–23 μm in stomatal region and gradually enlarging posterior to be double well developed pharyngeal bulbs (Figs. 1D, 2A, 2C). The pharyngeal posterior double bulb 45–69 μm, pear-shaped with a constriction to split it into two parts, anterior part width 27–39 μm and posterior part width 31–44 μm. Cardia small, surrounding by intestine. Ventral gland cell large, located posterior to the terminal pharyngeal bulb, excretory pore opening at the collar through a slender duct. Nerve ring located at 52%–57% of pharynx, 65–80 μm from anterior end. Two tail setae present, tail conical with prominent spinneret, length 114–144 μm. Spinneret finger-like, neither somatic setae exist nor annulated.

Male: reproductive system monorchic with outstretched testis located to the right of intestine. Spicules slender, arch-like, proximal with a slightly waved, middle curved, distal pointed, 33–43 μm length



Fig. 1. *Ptycholaimellus luoyang* sp. nov. A, adult male under stereo microscope; B, lateral view of head, showing cephalic setae and lateral differentiation; C, lateral view of male head end, showing S-shaped dorsal tooth; D, double pharyngeal bulbs; E, lateral view of male body part, showing spicules and gubernaculum; F, lateral view of female body part, showing vulva and reflexed ovaries; G, lateral view of juvenile without lateral differentiation. Scale bars, A = 200 μm; B, D, E, G = 20 μm; C = 10 μm; F = 100 μm.

along arc. Gubernaculum rod-like, length 12–17 μm (Figs. 1E, 2B). Precloacal supplements absent.

Female: reproductive system with two opposed, reflexed ovaries, the anterior one located to the right of intestine, and the posterior one to the left (Figs. 1F, 2E). The Vulva located approximate at 46.1%–47.6% body length from cephalic part.

Juvenile: length 461 μm , with maximum body diameter 29 μm ($a = 15.8$). Without lateral differentiation (Fig. 1G). Other main characteristics are shared with adult except reproductive system.

Distribution: *P. luoyang* sp. nov. occurs within the mangrove wetlands of the Luoyang River estuary, the Jiulong River estuary (Fujian Province), the Neilingding Futian National Nature Reserve, Shenzhen City

(Guangdong Province), and the Xinying Port, Danzhou City (Hainan Province) in China.

Ecological note: Due to the relationships between specific nematode and mangrove species, it is important to understand the dispersal mechanism of free-living marine nematodes and their impact on nutrient cycling in the food web. Hence, the composition of mangroves species was recorded from each sampling site. *Acanthus ilicifolius*, *Aegiceras corniculatum*, *Avicennia marina*, and *Kandelia obovata* were recorded in Luoyang River estuary, Quanzhou Bay, Fujian Province. *Kandelia obovata* was recorded in the Jiulong River estuary, Fujian Province. *Bruguiera gymnohiza*, *Kandelia obovata* and *Acanthus ilicifolius* were recorded in Guangdong Neilingding Futian National

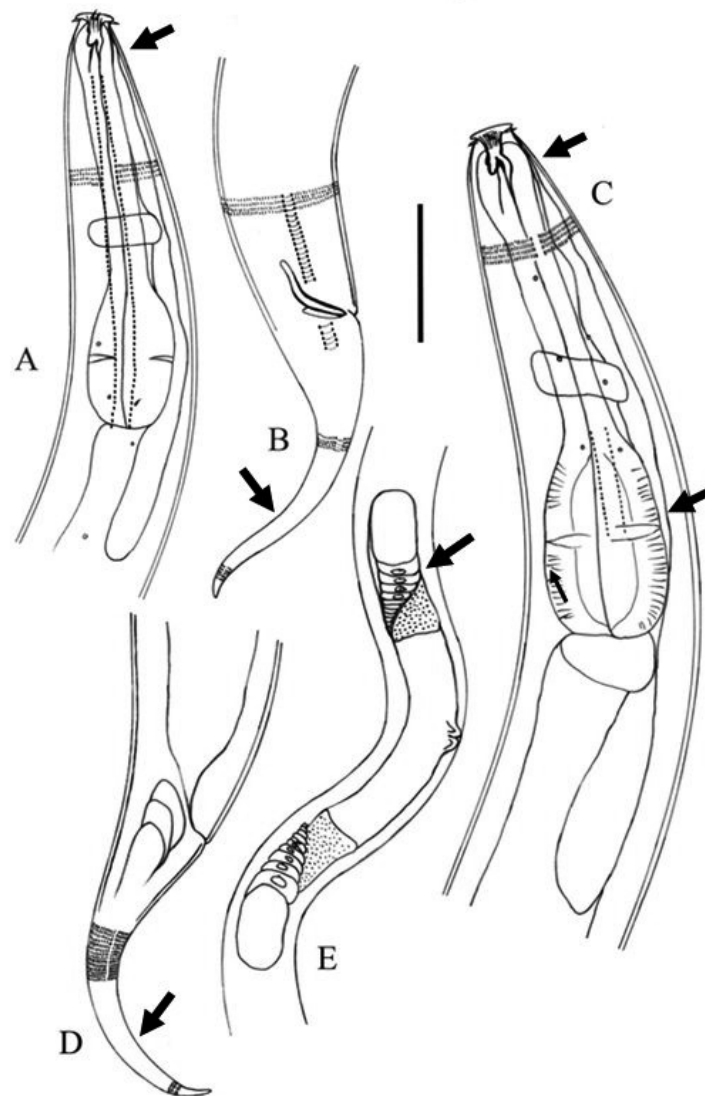


Fig. 2. *Ptycholaimellus luoyang* sp. nov. A, lateral view of male head end; B, lateral view of male tail region; C, lateral view of female head end and double pharyngeal bulbs; D, lateral view of female tail region; E: lateral view of female body part, showing ovaries. Scale bar: A–D = 50 μm ; E = 125 μm .

Nature Reserve, Shenzhen City, Guangdong Province. *Bruguiera sexangula* was recorded in Xinying Port, Danzhou City, Hainan Province.

DNA sequence results: A 294 base pair (bp) fragment of *COI*, a 264 bp fragment of 18S rDNA and a 302 bp fragment of 28S rDNA were used in this study. Therefore, the combined dataset consisted of 860 bp for phylogenetic analysis. “N” denotes a lack of fragments for said species. The Bayesian topology was identical for each species, strongly supporting monophyly with strong nodal support (0.99–1 posterior probability) (Fig. 3). The genetic results complement morphological evidence of *P. luoyang* sp. nov. being a distinct species. Interspecific and intrageneric thresholds of K2P distance divergence were as follows: 0–0.4% and 9.3%–18.4% for *COI*; 0 and 1.6%–4.4% for 18S rDNA; 0–1% and 8.9% for 28S rDNA, respectively.

Measurements: Holotype and a female paratype are present as follows. Detailed information of individual measurements are shown on the table 3.

Key to genus *Ptycholaimellus* Cobb, 1920 from China with the new species

- 1 Presence of ocelli at anterior end of body 2
- Absence of ocelli at anterior end of body 3
- 2 Cervical region abruptly narrowing, cephalic setae 1/4 h.d. long *P. ocellatus*
- Cervical region not abruptly narrowing, cephalic setae 2/3 h.d. long *P. adocius*
- 3 Body slimmer, width less than 50 μm 4
- Body stout, width more than 50 μm *P. luoyang* sp. nov.

- 4 Double pharyngeal bulb shorter than 40% of pharyngeal length .. 5
- Double pharyngeal bulb longer than 40% of pharyngeal length ... *P. longibulbus*
- 5 Cuticle with only two lateral longitudinal rows of double dots *P. macrodentatus*
- Cuticle with six longitudinal rows of double dots *P. pirus*

DISCUSSION

Ptycholaimellus luoyang sp. nov. differs from other species in its genus in having a pharynx cylindrical with anterior slightly swelling, possessing sclerotized transverse ridges occurring near the dorsal tooth, and through the structure of its spicules. The new species is distinguished from two similar species, *P. carinatus* and *P. slacksmithi* in having a body width exceeding 50 μm, but cephalic setae approximately 2 μm in length, amphid invisible (Huang and Gao 2016). Furthermore, it differs from its five Chinese congeners in the following ways: lacks ocelli, unlike *P. adocius* and *P. ocellatus* (Dashchenko and Belogurov 1984; Huang and Wang 2011); the length of the posterior pharynx bulb in relation to total pharynx length, compared to *P. longibulbus* (Wang, An and Huang, 2015); lacks precloacal supplement and amphids, unlike *P. macrodentatus*, plus the position of the testis differs (Timm 1961); the number of longitudinal rows of laterally differentiated cuticle punctations, compared to *P. pirus* (Huang & Gao, 2016). The identifiable characteristics for the above species are listed in table 4.

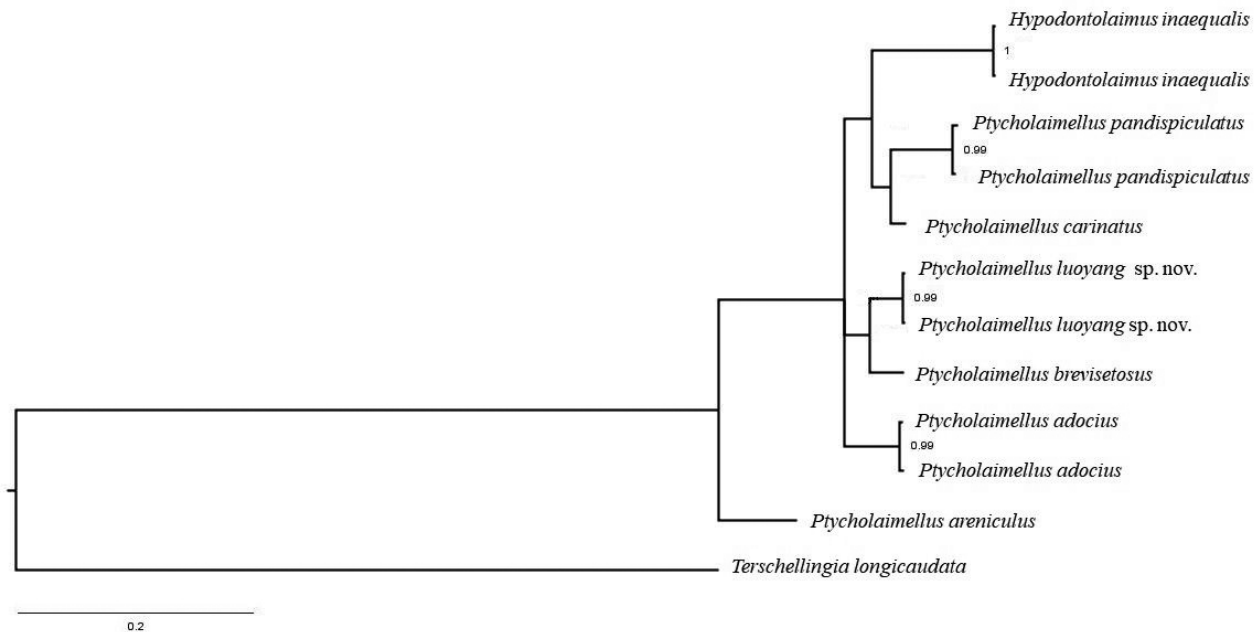


Fig. 3. Phylogenetic tree from MrBayes analysis of combined data set (860 bp from three genes). The branches of the new species are strongly supported by BI (PP > 0.90).

Table 3. Individual measurements of *Ptycholaimellus luoyang* sp. nov.

Specimen	Holotype				Paratype			
	♂ 1	♂ 2	♂ 3	♂ 4	♂ 5	♀ 1	♀ 2	Juv.1
Total body length	865	1177	1079	1220	1229	1130	1058	461
Maximum body diameter	55	60	56	71	77	69	60	29
Head diameter	12	15	14	17	17	16	15	10
Cephalic setae length	1.9	2.3	2.1	2.2	2.3	2.2	2.1	1.6
Nerve ring from anterior end	87	102	94	102	102	100	92	47
Nerve ring c.d.	38	46	41	49	46	53	46	22
Pharynx length	147	181	180	182	191	186	163	106
Pharynx c.d.	45	51	51	62	62	62	52	27
Posterior double bulb length	48	63	59	56	56	69	45	30
Anterior bulb width	27	31	28	33	29	39	32	23
Posterior bulb width	30	35	32	37	37	44	35	26
Spicule length as chord	30	37	36	40	37	-	-	-
Spicule length as arch	33	39	40	43	40	-	-	-
Gubernaculum length	12	13	14	17	13	-	-	-
a.b.d.	31	32	30	34	35	32	28	17
Tail length	114	121	120	131	116	118	144	77
Tail length/a.b.d	3.6	3.8	4.0	3.9	3.3	3.7	5.1	4.6
Vulva from anterior end	-	-	-	-	-	539	489	-
Vulva c.d.	-	-	-	-	-	66	57	-
V%	-	-	-	-	-	47.6	46.1	-
a	15.7	19.6	19.3	17.2	15.9	16.4	17.6	15.8
b	5.9	6.5	6.0	6.7	6.4	6.1	6.5	4.4
c	7.5	9.7	9.0	9.3	10.6	9.6	7.4	6.0

Table 4. Identifiable characteristics for *Ptycholaimellus luoyang* sp. nov. and seven other species

Species \ Characteristic	<i>Ptycholaimellus Luoyang</i> sp. nov.		<i>P. adocius</i>		<i>P. carinatus</i>		<i>P. longibulbus</i>	
	♂	♀	♂	♀	♂	♀	♂	♀
Specimen sexual	♂	♀	♂	♀	♂	♀	♂	♀
Length of cephalic setae	2		-		-		9	
Maximum body diameter	56–77	60–69	31.8–33.6	35.4	-	-	48–53	45
Ocelli	absent		present		absent		absent	
Length of the posterior pharynx bulb/pharynx length	33%	28–37%	-	-	36%		44–49%	
Precloacal supplement	absent	-	absent	-	absent	-	absent	-
Amphid	Invisible		Invisible		Half-moon shaped		Invisible	
Spicules	Slender, arch-like, proximal slightly waved, middle curved, distal pointed		Slightly arcuate		Broad, slightly cephalated		Arcuate	
Rows of lateral differentiation	Two		Two		Two		Two	

Species \ Characteristic	<i>P. macrodentatus</i>		<i>P. ocellatus</i>		<i>P. pirus</i>		<i>P. slacksmithi</i>	
	♂	♀	♂	♀	♂	♀	♂	♀
Specimen sexual	♂	♀	♂	♀	♂	♀	♂	♀
Length of cephalic setae	8		3	-	10–12	10–11	20–22	21–22
Maximum body diameter	-	-	29–32	32–37	22–25	32	51–52	75–80
Ocelli	absent		present		absent		absent	
Length of the posterior pharynx bulb/pharynx length	37.5%		26%		26–30%		-	-
Precloacal supplement	Present (2)	-	absent	-	absent	-	-	-
Amphid	Elliptical		Invisible		Invisible		Invisible	
Spicules	Extremely arcuate, slightly cephalated		Arcuate, proximal cephalated		Slender, strongly curved		Evenly curved, taper posteriorly to finely rounded ends	
Rows of lateral differentiation	Two		Two		Six		Two	

Regarding phylogenetic analyses, the genes are suitable for resolution at different taxonomic levels. 18S rDNA and 28S rDNA possess good resolution for identification at higher taxonomic rankings such as to separate the allied genera, while *COI* is a useful gene for identification at the species level (Deryckes et al. 2010; Sahraean et al. 2017). Although Bayesian topology suggested that the combined genes were useful for identification at the species level, it could not be elucidated to identify at the genus level in our study. This was caused by two main limitations: (1) nematode reference sequences were underpopulated in databases (Pitusi et al. 2021); (2) only six species of *Ptycholaimellus* and limited outgroup species were selected for phylogenetic analysis. Increasing the number of taxa for analysis would clarify phylogenetic relationships at both the genus and species levels (Bik et al. 2010).

The nucleotide divergence of genes could be used as a diagnostic tool for the discrimination of nematode species (Deryckes et al. 2010; Pitusi et al. 2021). Derycke et al. (2010) suggested that the intraspecific threshold was approximately 0.05 K2P distance for the *COI* gene. However, these data are incomplete for nematodes at present, and an intraspecific threshold is yet to be defined. Therefore, further study on the divergence of different species is necessary. In the present work, we determined the interspecific and intrageneric thresholds for the *COI*, 18S rDNA, and 28S rDNA genes, serving as a foundation for further study.

CONCLUSIONS

Ptycholaimellus is a cosmopolitan genus of free-living marine nematodes, highly abundant in mangrove wetlands. Here, a new species is described based on morphological characteristics and the *COI*, 18S rDNA, and 28S rDNA genes. *Ptycholaimellus luoyang* sp. nov. was distinguished from allied species owing to its short cephalic setae, pharynx cylindrical with anterior slightly swelling, sclerotized transverse ridges occurring near the dorsal tooth, and distally pointed spicules. Results from the phylogenetic analyses were regarded as morphological evidence to support the placement of the new species. Thus far, 23 species in the genus *Ptycholaimellus* have been identified. This study contributes toward our understanding of marine free-living nematodes, their diversity, and their functional roles within mangrove ecosystems.

Acknowledgments: This work and the new species name were registered with ZooBank under urn:lsid:zoobank.org:pub:10A31BE3-3A51-4310-

AF93-F1C82021DACB. This work was partially supported by a research grant from National Natural Science Foundation of China (Project no. 31772416). The authors would like to thank Zou MM, Pan C, and Zhu HL for sample collection. We also thank to the reviewers for their constructive criticism and improvement of the manuscript.

Authors' contributions: Shih YJ analysed the DNA data, drafted the manuscript and submitted the manuscript. Chen YZ gave a line-drawing and manuscript of diagnosis. Guo YQ designed this study and conducted the examination of morphological characteristic and reviewed the manuscript. All authors are in agreement with the content of the manuscript.

Competing interests: Shih YJ, Chen YZ and Guo YQ declare that they have no competing interests.

Availability of data and materials: Holotype and paratype have been deposited at the Fisheries College, Jimei University, Xiamen, China. The DNA sequence have been deposited in the GenBank database.

Consent for publication: Not applicable.

Ethics approval consent to participate: Not applicable.

REFERENCES

- Bhadury P, Austen MC, Bilton DT, Lamshead PJD, Rogers AD, Smerdon GR. 2006. Development and evaluation of a DNA-barcoding approach for the rapid identification of nematodes. *Mar Ecol Prog Ser* **320**:1–9. doi:10.3354/meps320001.
- Bhadury P, Austen MC, Bilton DT, Lamshead PJD, Rogers AD, Smerdon GR. 2008. Evaluation of combined morphological and molecular techniques for marine nematode (*Terschellingia* spp.) identification. *Mar Biol* **154**:509–518. doi:10.1007/s00227-008-0945-8.
- Bik HM, Lamshead PJD, Thomas WK, Lunt DH. 2010. Moving towards a complete molecular framework of the Nematoda: a focus on the Enoplida and early-branching clades. *BMC Evol Biol* **10**:353. doi:10.1186/1471-2148-10-353.
- Blaxter ML, DeLey P, Garey JR, Liu LX, Scheldeman P, Vierstraete A, Vanfleteren JR, Mackey LY, Dorris M, Frisse LM, Vida JT, Thomas WK. 1998. A molecular evolutionary framework for the phylum Nematoda. *Nature* **392**:71–75. doi:10.1038/32160.
- Dashchenko OI, Belogurov. 1984. The morphology of *Ptycholaimellus adocius* sp. n. (Nematoda, Chromadorida) from sponges of Posjet Bay, Sea of Japan. *Zool Zh* **63**:976.
- De Ley P, De Ley IT, Morris K, Abebe E, Mundo-Ocampo M, Yoder M, Heras J, Waumann D, Rocha-Olivares A, Burr AHJ, Baldwin JG, Thomas WK. 2005. An integrated approach to fast and informative morphological vouchering of nematodes for applications in molecular barcoding. *Phil Trans R Soc B* **360**:1945–1958. doi:10.1098/rstb.2005.1726.

- Derycke S, Vanaverbeke J, Rigaux A, Backeljau T, Moens T. 2010. Exploring the use of cytochrome oxidase *c* subunit 1 (*COI*) for DNA barcoding of free-living marine nematodes. *PLoS ONE* **5**:e13716. doi:10.1371/journal.pone.0013716.
- Ferris H. 2010. Contribution of nematodes to the structure and function of the soil food web. *J Nematol* **42**:63–67.
- Guo YQ, Chang Y, Chen YZ, Li YX, Liu AY. 2015. Description of a marine nematode *Hopperia sinensis* sp. nov. (Comesomatidae) from mangrove forests of Quanzhou, China, with a pictorial key to *Hopperia* species. *J Ocean Univ China* **14**:1111–1115. doi:10.1007/s11802-015-2742-6.
- Huang Y, Gao Q. 2016. Two new species of Chromadoridae (Chromadorida: Nematoda) from the East China Sea. *Zootaxa* **4144**:89–100. doi:10.11646/zootaxa.4144.1.4.
- Huang Y, Wang JY. 2011. Two new free-living marine nematode species of Chromadoridae (Nematoda: Chromadorida) from the Yellow Sea, China. *J Nat Hist* **45**:2191–2201. doi:10.1080/00222933.2011.591510.
- Jensen P, Nehring S. 1992. Review of *Ptycholaimellus* Cobb (Nematoda, Chromadoridae), with descriptions of three species. *Zool Scr* **21**:239–245. doi:10.1111/j.1463-6409.1992.tb00327.x.
- Leduc D, Zhao ZQ. 2021. Molecular characterization of free-living nematodes from Kermadec Trench (Nematoda: Aegialoalaimidae, Xyalidae) with description of *Aegialoalaimus tereticauda* n. sp. *Zootaxa* **4949**:341–352. doi:10.11646/zootaxa.4949.2.7.
- Mokievsky VO, Tchesunov AV, Udalov AA, Toan ND. 2011. Quantitative distribution of meiobenthos and the structure of the free-living nematode community of the mangrove intertidal zone in Nha Trang bay (Vietnam) in the South China Sea. *Russ J Mar Biol* **37**:272–283. doi:10.1134/S1063074011040109.
- Naidoo G, Naidoo K, Swart A. 2021. Oil Pollution Effects on Nematodes in Mangrove Sediment: A Microcosm Study. Preprint (Version 1) at Research Square. doi:10.21203/rs.3.rs-749759/v1.
- Nicholas WL, Elek JA, Stewart AC, Marples TG. 1991. The nematode fauna of a temperate Australian mangrove mudflat; its population density, diversity and distribution. *Hydrobiologia* **209**:13–27. doi:10.1007/BF00006714.
- Pitussi V, Søreide JE, Hassett BT, Marquardt M, Andreassen MH. 2021. The occurrence of *Nematoda* in coastal sea ice on Svalbard (European Arctic) determined with the 18S small subunit rRNA gene. *Polar Biol* **44**:1153–1162. doi:10.1007/s00300-021-02863-y.
- Ridall A, Ingels J. 2021. Suitability of free-living marine nematodes as bioindicators: Status and future considerations. *Front Mar Sci* **8**:1–16. doi:10.3389/fmars.2021.685327.
- Rzeznik-Orignac J, Fichet D, Boucher G. 2003. Spatio-temporal structure of the nematode assemblages of the Brouage mudflat (Marennes Oléron, France). *Estuar Coast Shelf Sci* **58**:77–88. doi:10.1016/S0272-7714(03)00061-1.
- Sahraean N, Van Campenhout J, Rigaux A, Mosallanejad H, Leliaert F, Moens T. 2017. Lack of population genetic structure in the marine nematodes *Ptycholaimellus pandispiculatus* and *Terschellingia longicaudata* in beaches of the Persian Gulf, Iran. *Mar Ecol* **38**:e12426. doi:10.1111/maec.12426.
- Timm RW. 1961. The marine nematodes of the Bay of Bengal. *Proc Pakistan Acad Sci* **1**:25–88.
- Wang CM, An LG, Huang Y. 2015. A new species of free-living marine nematode (Nematoda: Chromadoridae) from the East China Sea. *Zootaxa* **3947**:289–295. doi:10.11646/zootaxa.3947.2.11.
- Yang PP, Chang Y, Guo YQ, Chen CC. 2019. Dominant genera of marine nematodes and their feeding types in several mangrove wetlands of Fujian Province. *Haiyang Xuebao* **41**:90–102. (in Chinese)
- Yang PP, Liu MD, Guo Y. 2020. One new species and one new record species of *Sphaerolaimus* (Nematode, Sphaerolaimidae) in offshore wetlands, China. *J Ocean Limnol* **39**:683–692. doi:10.1007/s00343-020-9292-5.